A High-Speed Stereo Matching Algorithm Based on Synergetics

Tohru Irie*, Tomohito Murakami**, Hiroshi Maeda* and Norikazu Ikoma*

*Dept. of Computer Engineering, Faculty of Engineering, Kyushu Institute of Technology,
1-1 Sensuicho, Tobata, Kitakyushu, 804-8550, Japan

**Hitachi, Ltd., 4-6, Kanda Surugadai, Chiyoda, Tokyo 101-8010, Japan

email:irie@sys2.comp.kyutech.ac.jp

***Abstract*--A pattern recognition algorithm based on Synergetics is applied to match stereo images. This algorithm needs to numerically solve differential equations called order parameter equations. Thus, this method had a high-matching precision but much computation time. This paper proposes a high-speed stereo matching algorithm without loss of matching precision. The algorithm is developed by the way without solving the order parameter equations directly.**

I. INTRODUCTION

3-D reconstruction from stereo images is one of the most typical problems in computer vision. The main issue in processing stereo images is to decide the correspondence points between a left image and a right image, that is, a stereo matching problem. Stereo matching on the images including occlusion and reversal position is still a remained difficult problem. Although many methods [1] have been proposed for solving this problem, efficient and effective method is not explored yet.

For the problem, We proposed a new stereo matching algorithm [2] using the pattern recognition based on Synergetics proposed by H.Haken [3]. This method needed to numerically solve differential equations called order parameter equations, which have two kinds of parameters, order parameter and attention parameter. Thus, this method had high matching precision but required much computation time.

In this paper, we propose a high-speed stereo matching algorithm that can judge the correspondence points only by initial values of order parameters and attention parameters, namely without solving the differential equations.

Chapter II describes the outline of the stereo matching algorithm that used Synergetics. Chapter III analyzes the meaning of the order parameter equation and, thereby, constitutes the high-speed algorithm. Chapter IV compares the previous method and the proposed method in computation time and matching precision. Chapter V is conclusive remarks.

II. OUTLINE OF A STEREO MATCHING ALGORITHM BASED ON SYNERGETICS

A. Outline of Synergetics

A certain state in a dynamical system autonomously changes to another ordered state by external controls or fluctuation forces. This process is called self-organization. Synergetics explains self-organization as follows: When a system receives an external environmental change, the system prepares stable modes and unstable modes for the reconstruction of its state. The stable modes are dominated by the unstable modes, and then vanish. This mechanism is called a slaving principle of Synergetics. The unstable modes are the candidates for a future ordered state in the system. A specific unstable mode wins the growing competition among the modes, and then forms a new ordered state in the system. The equations representing this competition are called order parameters equations of Synergetics.

Let us consider an autonomous system equation (1) with an external control parameter α and nonfluctuation force and a state vector be $\boldsymbol{q}(\boldsymbol{x}, t)$,

$$\dot{\boldsymbol{q}} = \boldsymbol{N}(\boldsymbol{q}(\boldsymbol{x},t),\alpha)\ . \tag{1}$$

After this, $\boldsymbol{q}(\boldsymbol{x}, t)$ is written in $\boldsymbol{q}$ for simplicity. Furthermore, let us suppose equation (1) has a stable solution $\boldsymbol{q}_0$ for a certain value of α and then $\boldsymbol{q} = \boldsymbol{q}_0 + \boldsymbol{w}(\boldsymbol{x}, t)$, where $\boldsymbol{x}$ is a position vector, and $\boldsymbol{w}$ represents a small change. Here, expanding $\boldsymbol{N}$ in a power series around $\boldsymbol{q}_0$,

$$\dot{\boldsymbol{q}} = \boldsymbol{N}(\boldsymbol{q}_0) + \boldsymbol{L}\boldsymbol{w} + \hat{\boldsymbol{N}}(\boldsymbol{w})\ . \tag{2}$$

Here, the third term of right-hand side contains the second and / or higher powers of $\boldsymbol{w}$. Furthermore, disregarding terms of more than second orders and adjusting the scale $\boldsymbol{N}(\boldsymbol{q}_0)=0$, (2) is transformed into

$$\dot{\boldsymbol{w}} = \boldsymbol{L}\boldsymbol{w}\ ,\ \boldsymbol{L} = (L_{ij}) = (\partial N_i / \partial q_j \mid \boldsymbol{q} = \boldsymbol{q}_0)\ . \tag{3}$$

The solutions of (3) can be written in the general form

$$\boldsymbol{w}(\boldsymbol{x},t) = e^{\lambda t}\boldsymbol{v}(\boldsymbol{x})\ . \tag{4}$$

In the case of nondegenerate eigenvalues, let us suppose the state vector $\boldsymbol{q}$ is presented as

$$\boldsymbol{q} = \boldsymbol{q}_0 + \sum_j \xi_j(t)\boldsymbol{v}_j(\boldsymbol{x})\ ,\ \xi_j(t) = A_j e^{\lambda_j t}\ . \tag{5}$$

Here, λ_j and $\boldsymbol{v}_j$ are the j-th eigenvalue and its eigenvector. Now, a set of adjoint vector $\boldsymbol{v}^+_k$, which satisfies an orthogonal condition, is introduced. The symbol < > means inner product.

$$< \boldsymbol{v}_k^+ \boldsymbol{v}_i > = \delta_{ki}\ ,\ \delta_{ki} = \begin{cases} 1 & for\quad k = i, \\ 0 & otherwise\ . \end{cases} \tag{6}$$

Then, inserting (5) into (2) and multiplying (2) by $\boldsymbol{v}^+_k$,

$$\boldsymbol{v}_k^+ \sum_j \dot{\xi}_j(t)\boldsymbol{v}_j = \boldsymbol{v}_k^+ \sum_j \xi_j(t)\boldsymbol{L}\boldsymbol{v}_j + \boldsymbol{v}_k^+ \hat{\boldsymbol{N}}(\sum_j \xi_j(t)\boldsymbol{v}_j)\ . \tag{7}$$

From (6), the following is obtained.

$$\dot{\xi}_k = \lambda_k \xi_k + \tilde{N}_k(\xi_j)\ . \tag{8}$$

Equations (8) are divided into two set of unstable modes (the real part of eigenvalue is non-negative) and stable modes (the real part of eigenvalue is negative). Applying the slaving principle here, the stable modes are represented by the unstable modes and eliminated from (8). Consequently, the following order parameter equations of Synergetics

$$\xi_k = \lambda_k \xi_k - B\sum_{k' \neq k} \xi_{k'}^2 \xi_k - C(\sum_{k'} \xi_{k'}^2)\xi_k\ ,\ k = 1,\ldots,N \tag{9}$$

are led, where B and C are positive constants, and ξ_k and λ_k are called order parameter and attention parameter, respectively. The initial value of order parameter is given with an inner product.

$$\xi_k(0) = < \boldsymbol{v}_k^+ \boldsymbol{q}(0) >\ . \tag{10}$$

One of ξ_k's survives, namely, grows to a positive value, in (9) and forms a new ordered state in the system.

In the application of equation (9) to pattern recognition, $\boldsymbol{q}$ and $\boldsymbol{v}_k$ correspond to an input pattern vector and the k-th prototype pattern vector, respectively. Thus, ξ_k represents a kind of similarity between an input pattern vector and the k-th prototype vector. λ_k plays a roll to control the increase of ξ_k. In equation (9), a surviving order parameter converges to a positive value and the others converge to 0. This means, from equation (5), the prototype pattern corresponding to the index of the surviving order parameter is recognized.

B. *Outline of Stereo Matching Algorithm*

This section describes the application of Synergetics to a stereo matching problem. This paper considers the following stereo vision system:

a) Camera geometry is parallel as shown in Fig.'s 1(a) and (d), so that epipolar lines are parallel with X-axis in a camera coordinate system (Fig.'s 1(b), (c), (e), and (f)).

b) The object of stereo vision is building blocks.

c) Feature points are the edges of the building blocks and obtained by Smooth filter of 3×3 pixels window, Laplacian operator of a 3×3 pixels window, and the Thinning operator of a 3×3 pixels window.

d) Matching primitives are edge points as shown in Fig.'s 1(b), (c), (e), and (f), where occlusion (a point C) appears in the right image (Fig. 1(c)), and reversal position (points G, H, and I) appears in the both image (Fig.'s 1(e) and (f)).

Hence, stereo images generally include occlusion and reversal position. The stereo images with occlusion have feature points not to be match. And the stereo image with reversal position cannot obtain correct correspondence by the method based on Markov condition such as DP-matching. Then, we take a two-stage matching approach. In the first stage, the feature points to be obviously corresponded are found. Here, it is expected the occluded feature points are not corresponded. The remaining points are matched in the second stage.

In a stereo matching problem, we assign an input pattern vector on an edge point in one image to $\boldsymbol{q}$ and do the k-th prototype pattern vector on edge points in the other image to $\boldsymbol{v}_k$.

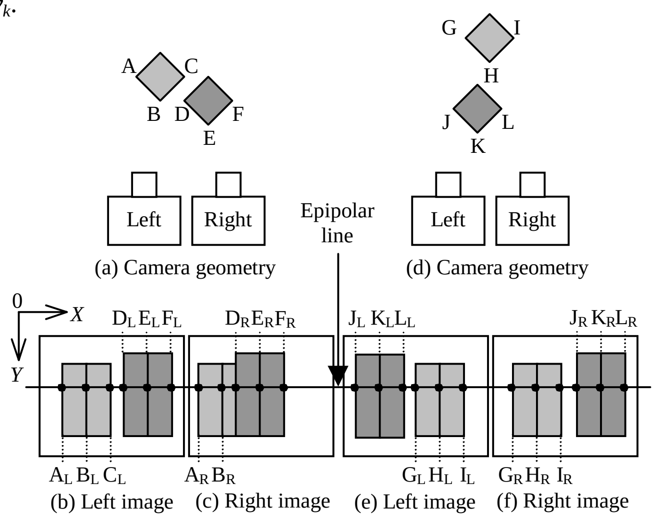

Fig. 1. Stereo matching

The elements of pattern vector and attention parameter used in each stage is described below.

1) Elements of pattern vector

We adopted the following elements as the pattern vector in the first and the second stage:

a) Brightness values of pixels of four area windows (small 7×7, large 7×5 of 3×5 unit, perpendicular 1×48, and both ends area of edge a couple of 11×11).

b) Length and angle of an edge sequence, which extends in direction of Y-axis from the current edge.

Therefore, pattern vector has the pixel elements of *a)* and *b).*

2) Elements of attention parameter

The following elements are adopted as the determination of an attention parameter:

a) Brightness values of pixels of two area windows (horizontal 106×1 and perpendicular 1×240).

b) Average brightness of pixels of small area window.

c) Information about position of the feature point on the image.

d) Information about distance to the neighborhood edge of the feature point.

e) Length and angle of an edge sequence, which extends in the direction of Y-axis from the current edge.

Here, similarity between an input pattern and a prototype pattern is defined with respect to five elements *a)-e)*, and the attention parameter is set up by the weighted sum of similarities.

Let's consider a case where two candidates ($\boldsymbol{v}_1$ and $\boldsymbol{v}_2$) for correspondence point to an input pattern exist. This is the case of N=2 (B=1 and C=1) in (9), and is as follows:

$$\dot{\xi}_1 = -\xi_1(\xi_1^2 + 2\xi_2^2 - \lambda_1)\,. \quad (11)$$

$$\dot{\xi}_2 = -\xi_2(\xi_2^2 + 2\xi_1^2 - \lambda_2)\,. \quad (12)$$

The initial values of order parameters obtained by (10) and the attention parameters are substituted for (11) and (12). And Fig. 2 shows the dynamics of the order parameters, where $\xi_1(0)$=0.5, $\xi_2(0)$=0.6, λ_1=1.0 and λ_2=0.8. This case shows that ξ_1 grew to 1, namely pattern $\boldsymbol{v}_1$ is recognized. Thus, the previous method needed to solve the order parameter equations numerically.

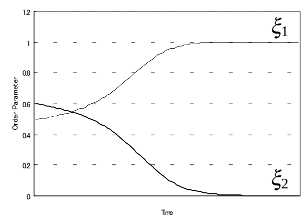

Fig. 2. Order parameter ($\xi_1(0)$=0.5, $\xi_2(0)$=0.6, λ_1=1.0, λ_2=0.8, N=2)

III. Analysis Of Order Parameter Equation, And High-Speed Algorithm

In this section, the meaning of the order parameter equations is analyzed in more detail, and a high-speed algorithm is derived

A. *Analysis of meanings of the order parameter equations*

Firstly, let us consider the order parameter equations of two dimensions, namely (11) and (12). We can find the singular points ξ_1, ξ_2 of real number at $\dot{\xi}_1 = \dot{\xi}_2 = 0$, and obtain the following four cases.

(i) Unstable focus P_0 $\xi_1 = \xi_2 = 0$. (13)

(ii) Stable focus P_1 $\xi_1 = \pm\sqrt{\lambda_1}$, $\xi_2 = 0$. (14)

(iii) Stable focus P_2 $\xi_1 = 0$, $\xi_2 = \pm\sqrt{\lambda_2}$. (15)

(iv) Saddle point P_s $\xi_1 = \pm\sqrt{\frac{2\lambda_2 - \lambda_1}{3}}$, $\xi_2 = \pm\sqrt{\frac{2\lambda_1 - \lambda_2}{3}}$. (16)

These singular points are shown in Fig. 3. In the following, we discuss only the first quadrant because singular points are symmetry. Here, a potential function is introduced in order to clarify the meaning of the singular points. Potential function V is defined by

$$\dot{\xi}_k = -\frac{\partial V}{\partial \xi_k} . \qquad (17)$$

Using (17) and (9), we find

$$V = -\frac{1}{2}\sum_{k=1}^{N}\lambda_k \xi_k^2 + \frac{1}{4}B\sum_{k' \neq k}^{N}\xi_{k'}^2\xi_k^2 + \frac{1}{4}C(\sum_{k'=1}^{N}\xi_{k'}^2)^2 . \qquad (18)$$

Now we consider two dimensions, namely N=2, then

$$V = -\frac{1}{2}(\lambda_1\xi_1^2 + \lambda_2\xi_2^2) + \frac{1}{2}\xi_1^2\xi_2^2 + \frac{1}{4}(\xi_1^2 + \xi_2^2)^2 . \qquad (19)$$

The contour map and the landscape of potential (19) are shown in Fig. 4(a) and Fig. 4(b), where λ_1=1.0 and λ_2=0.8, for instance, and a saddle point, stable focuses, unstable focuses are shown as symbols △, ○, □. The order parameter equations (11) and (12) represent the motion of a particle on a potential surface. If the initial values of the k-th order parameter is given as the location X in Fig. 4(a), the particle which corresponds to the value of order parameter, roles down on the potential surface and settles in one stable focus (ξ_1=1). Since this stable focus is corresponding to a prototype pattern, the corresponding pattern is recognized as $\boldsymbol{v}_1$. At this time the ridge of potential, which is represented by the line through □ to △ in Fig. 4(a), is the watershed to determine which stable focus is chosen. Thus, if we can approximate this ridge that passed from the origin (unstable focus) to the saddle point, the recognized pattern can be easily judged only by the initial values of the order parameters.

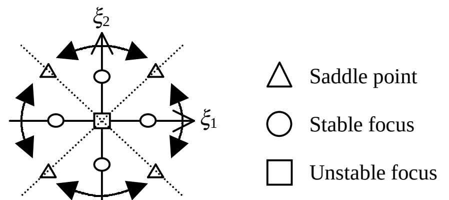

Fig. 3. Configuration of singular point (2-D)

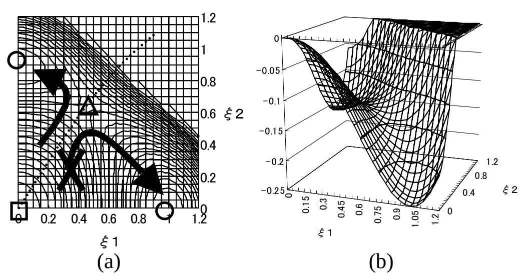

Fig. 4. Potential function (λ_1=1.0, λ_2=0.8)

Thus, the position and the property of the singular points are important in the order parameter equations. Since the order parameter equations cannot be solved directly, we represent those with the first-order approximation using jacobian and analyze the orbits of the solutions near the singular points. Linear expression of (11) and (12) is

$$\begin{pmatrix}\dot{\xi}_1 \\ \dot{\xi}_2\end{pmatrix} = \boldsymbol{A}\begin{pmatrix}\xi_1 \\ \xi_2\end{pmatrix} . \qquad (20)$$

where $\boldsymbol{A}$ is Jacobian and is expressed with

$$\boldsymbol{A} = \begin{pmatrix} a_{11} & a_{12} \\ a_{21} & a_{22}\end{pmatrix}, \quad a_{ij} = \left.\frac{\partial F_i}{\partial \xi_j}\right|_{\xi_1=\xi_2=0} \quad (i, j = 1, 2)$$, and then

$$\boldsymbol{A} = \begin{pmatrix} -3\xi_1^2 - 2\xi_2^2 + \lambda_1 & -4\xi_1\xi_2 \\ -4\xi_1\xi_2 & -2\xi_1^2 - 3\xi_2^2 + \lambda_2 \end{pmatrix} . \qquad (21)$$

The property of the singular points is specified by the eigenvalues of $\boldsymbol{A}$. Let us be $0 \le \lambda_1, \lambda_2 \le 1$ without the loss of generality. In a case of two dimensions, if both of the eigenvalues e_1 and e_2 at a singular point are positive real numbers, the orbit of the solution grows away from the singular point. This singular point is an unstable focus. Conversely, if both of the eigenvalues are negative real numbers, it is a stable focus, and the orbit of the solution approaches the singular point. And the case of $e_1 \times e_2 < 0$, the singular point is a saddle point. Table I shows the properties of the singular points and the corresponding conditions of the eigenvalues. Now, we analyze the singular points P_0, P_1, P_2 and P_s by using the eigenvalues . Here, in the case of $\lambda_1 = \lambda_2 = 0$, all the singular points become the same as the origin, and lead all the eigenvalues to 0. This is trivial and excepted from the consideration.

TABLE I SINGULAR POINT AND EIGENVALUE

Condition of Eigenvalue	Singular point
$e_1 > 0$, $e_2 > 0$	Unstable focus
$e_1 < 0$, $e_2 < 0$	Stable focus
$e_1<0$, $e_2>0$ ($e_1>0$, $e_2<0$)	Saddle point
$e_1<0$, $e_2=0$ ($e_1=0$, $e_2<0$)	Non-simple (NS) singular point

1) In case of $\boldsymbol{A}^{P_0}$

The coordinates of the singular point P_0 is given in (13), and the Jacobian at P_0 is

$$\boldsymbol{A}^{P_0} = \begin{pmatrix}\lambda_1 & 0 \\ 0 & \lambda_2\end{pmatrix} . \qquad (22)$$

Here, the eigenvalues e_1 and e_2 are calculated as $e_1 = \lambda_1 \ge 0$ and $e_2 = \lambda_2 \ge 0$. P_0 is an unstable focus.

2) In cases of $\boldsymbol{A}^{P_1}$ and $\boldsymbol{A}^{P_2}$

In the same manner, the Jacobian at P_1 and P_2 are

$$\boldsymbol{A}^{P_1} = \begin{pmatrix} -2\lambda_1 & 0 \\ 0 & -2\lambda_1 + \lambda_2\end{pmatrix}, \quad \boldsymbol{A}^{P_2} = \begin{pmatrix} -2\lambda_2 + \lambda_1 & 0 \\ 0 & -2\lambda_2\end{pmatrix} . \qquad (23)$$

Here, three cases exist for $\boldsymbol{A}^{P_1}$ and are summarized as follows (Note that $0 \le \lambda_1, \lambda_2 \le 1$):

(Stable focus P_1) $e_1 = -2\lambda_1 < 0$, $e_2 = -2\lambda_1 + \lambda_2 < 0$ (24)

(Saddle point P_1) $e_1 = -2\lambda_1 < 0$, $e_2 = -2\lambda_1 + \lambda_2 > 0$ (25)

(NS-singular points P_1) $e_1 = -2\lambda_1 < 0$, $e_2 = -2\lambda_1 + \lambda_2 = 0$ (26)

In the same manner, three cases for $\boldsymbol{A}^{P_2}$ are shown below.

(Stable focus P_2) $e_1 = -2\lambda_2 + \lambda_1 < 0$, $e_2 = -2\lambda_2 < 0$ (27)

(Saddle point P_2) $e_1 = -2\lambda_2 + \lambda_1 > 0$, $e_2 = -2\lambda_2 < 0$ (28)

(NS-singular points P_2) $e_1 = -2\lambda_2 + \lambda_1 = 0$, $e_2 = -2\lambda_2 < 0$ (29)

Here, the conditions are considered together about the singular points P_1 and P_2. In formula (24)-(26) and formula (27)-(29), $-2\lambda_1 < 0$ and $-2\lambda_2 < 0$ are clear from conditions $0 \le \lambda_1, \lambda_2 \le 1$. Therefore, either of the condition (30.a) or (30.b) is satisfied in (24) and (27).

$2\lambda_1 - \lambda_2 > 0$ …(a), $2\lambda_2 - \lambda_1 > 0$ …(b) (30)

And all the combinations of two singular points P_1 and P_2 are as follows:

a) Stable focus P_1 and stable focus P_2.
b) Stable focus P_1 and NS-singular point P_2. (And reverse.)
c) Stable focus P_1 and saddle point P_2. (And reverse.)

Here, *a)* is described in *3)*. And Fig.'s 5(a), (b) show the orbit of the solutions near these singular points in case of *c)* and *b)*, respectively.

3) In case of $\boldsymbol{A}^{P_S}$

The coordinates of the singular point P_s is given in (16), and the Jacobian at P_s of a saddle point,

$$\boldsymbol{A}^{P_S} = \begin{pmatrix} -\frac{2(2\lambda_2-\lambda_1)}{3} & -\frac{4\sqrt{(2\lambda_2-\lambda_1)(2\lambda_1-\lambda_2)}}{3} \\ -\frac{4\sqrt{(2\lambda_2-\lambda_1)(2\lambda_1-\lambda_2)}}{3} & -\frac{2(2\lambda_1-\lambda_2)}{3} \end{pmatrix} = \begin{pmatrix} -a & -c \\ -c & -b \end{pmatrix}. \quad (31)$$

The eigenvalues are calculated as follows:

$$e_1 = \frac{-(a+b)+\sqrt{(a+b)^2+12ab}}{2} > 0 \text{ , } e_2 = \frac{-(a+b)-\sqrt{(a+b)^2+12ab}}{2} < 0 \quad (32)$$

Here, since ξ_1 and ξ_2 are the real numbers $(\xi_1 > 0, \xi_2 > 0)$, it must satisfy (30). Hence a, b, and c are positive, and then $e_1 > 0$ and $e_2 < 0$. Namely, P_s is a saddle point. In this case, P_1 and P_2 are the stable focuses, and Fig. 5(c) shows these singular points. Here, the emphases are that 1) the change of the properties of P_1 and P_2 by the conditions, 2) the conditions in which P_s exists, 3) the position of the saddle point. The above main point is summarized as follows:

a) The singular points of order parameter equations are specified by the values of attention parameters.
b) The property of singular points is determined by the sign of eigenvalues of Jacobian $\boldsymbol{A}$, as shown in Table I.
c) When a saddle point exists, the ridge curve passing through origin to the saddle point determines which stable focus is recognized.

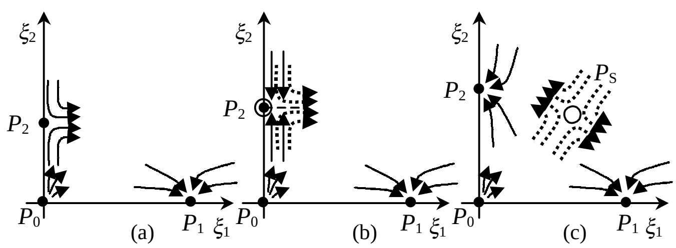

(a)	(b)	(c)
P_1: Stable focus	P_1: Stable focus	P_1: Stable focus
P_2: Saddle point	P_2: NS-singular point	P_2: Stable focus
P_0: Unstable focus	P_0: Unstable focus	P_s: Saddle point
		P_0: Unstable focus

Fig. 5. The orbit of the solution near each singular point

B. *In case of n Dimensions*

Secondly, the case of n dimensions is considered based on two-dimensions. Here, let us give some definitions and propositions.

[*Definition 1*]

A *n-dimensional* singular point is the point that satisfies $\dot{\xi}_1 = \dot{\xi}_2 = \cdots = \dot{\xi}_n = 0$ and $\forall i \quad \xi_i > 0$ in equation (9).

[*Definition 2*]

A *n*-(*k*)-*dimensional* singular point is the point that satisfies $\dot{\xi}_1 = \dot{\xi}_2 = \cdots = \dot{\xi}_n = 0$ and $\xi_i > 0$, $\xi_j = 0$, $(i = 1,\ldots,k, \ \ j = k+1,\ldots,n)$ in equation (9). Here, the index i that satisfies $\xi_i > 0$ is rearranged in small order, and the index j that satisfies $\xi_j = 0$ is also rearranged in small order.

[*Definition 3*]

A lower derivative singular point is the singular point that is produced by setting up $\xi_i > 0$ of a *n*-(*k*)-*dimensional* singular point to $\xi_i = 0$. Conversely, a upper derivative singular point is the singular point that is produced by setting up $\xi_i = 0$ of a *n*-(*k*)-*dimensional* singular point to $\xi_i > 0$.

[*Definition 4*]

A *n-dimensional* ridge hypersurface is the border hypersurface that is constructed by a hypercurve which connects origin to a *n-dimensional* singular point, and hypercurves which connect origin to *n*-(*n*-1)-*dimensional* singular points, and determines which order parameter grows to 1.

We consider the case where a *n-dimensional* singular point exists. If a *n-dimensional* singular point does not exist and a *n*-(*n'*)-*dimensional* singular point $(n' < n)$ exists, the following can be discussed without the loss of generality by replacing *n* for *n'*.

[*Proposition 1*]

A *n-dimensional* singular point exists, *iff* condition (33) is satisfied, and its coordinate is given as (34).

$$2\sum_{k \ne i}^{n} \lambda_k - (2n-3)\lambda_i > 0 , \quad (i = 1,2,\cdots n) . \quad (33)$$

$$\xi_i = \sqrt{\frac{2\sum_{k \ne i}^{n} \lambda_k - (2n-3)\lambda_i}{2n-1}} . \quad (34)$$

(Proof)

The following equation is obtained from (9) as $B = C = 1$.

$$\dot{\xi}_i = -\xi_i(2\xi_1^2 + 2\xi_2^2 + \cdots + \xi_i^2 + \cdots + 2\xi_n^2 - \lambda_i) , \ (i = 1,2,\cdots n) . \quad (35)$$

From (35), $\dot{\xi}_i = 0$ and $\xi_i > 0$,

$$2\xi_1^2 + 2\xi_2^2 + \cdots + \xi_i^2 + \cdots + 2\xi_n^2 - \lambda_i = 0 , \ (i = 1,2,\cdots n) . \quad (36)$$

By solving simultaneous equations (36), (33) and (34) are obtained. Detailed derivation is omitted.

(End of proof)

We present the following propositions without proofs.

[*Proposition 2*]

If a *n-dimensional* singular point exists, *n*-(*n*-1)-*dimensional* lower derivative singular points exist.

[*Proposition 3*]

If a *n*-(*n*-1)-*dimensional* singular point doesn't exist, *n-dimensional* upper derivative singular point doesn't exist.

[*Proposition 4*]

If a n-(k-1)-*dimensional* singular point doesn't exist, n-(k)-*dimensional* upper derivative singular point doesn't exist.

[*Proposition 5*]

If a *n-dimensional* singular point exists, the eigenvalues of Jacobian ***A*** have (n-1) positive real numbers and one negative real number.

[*Proposition 6*]

If a *n-dimensional* singular point exists, the eigenvalues of Jacobian ***A*** of n-(n-1)-*dimensional* lower derivative singular points have two negative real numbers.

[*Proposition 7*]

If a n-(k)-*dimensional* singular point exists, the eigenvalues of Jacobian ***A*** of n-(k-1)-*dimensional* lower derivative singular points have at least two negative real numbers.

[*Theorem 1*]

If formula (33) is not satisfied in an index i^*, one of the lower derivative n-(k)-*dimensional* singular points $(\xi_{i^*}=0,\ k=0,\ldots,n-1)$ has the same combination of signs as the signs of eigenvalues of *n-dimensional* singular point. Here, "the same combination of signs as the signs of eigenvalues" is (n-1) positive real numbers and one negative real number.

Here, the elements of Jacobian in n dimensions are expressed as follows:

$$a_{ij}=\begin{cases}-2\sum_{p=1}^{n}\xi_p^2-\xi_i^2+\lambda_i & (i=j)\\ -4\xi_i\xi_j & (i\neq j)\end{cases} \tag{37}$$

Then, we present the approximate construction of ridge hypersurface as follows:

1) When a n-dimensional singular point exists

In this case, all the n-(k)-*dimensional* singular points $(k=0,\ldots,n-1)$ exist by ***Proposition 2***. Then, the ridge hypersurfaces between n and (n-1) dimensions are approximately consisted of connecting the following hypercurves (***Theorem 1***).

a) The hypercurve that connects *n-dimensional* singular point and origin.

b) The hypercurves that connect n-(n-1)-*dimensional* singular points and origin.

And the ridge hypersurface between k and (k-1) dimensions are approximately consisted in a similar manner.

2) When a n-(k)-dimensional singular point doesn't exist

In this case, a n-(k-1)-*dimensional* singular point exists, and all the n-(k-2)-*dimensional* lower derivative singular points exist by ***Proposition 2***. Then, the ridge hypersurfaces are approximately consisted of connecting the following hypercurves. And the ridge hypersurfaces in (k-2) dimensions or lower dimensions are done in the same manner as *1)* (***Theorem 1***).

a) The hypercurve that connects a singular point which has the same combination of signs as the signs of eigenvalues of a *n-dimensional* singular point, and origin.

b) The hypercurves that connect singular points which have the same combination of signs as the signs of eigenvalues of n-(n-1)-*dimensional* singular points, and origin.

C. High-Speed Algorithm

Finally, a high-speed algorithm is constructed here. Now, we consider the case where *n-dimensional* singular point exists, and search by n-(k)-*dimensional* singular points $(k=2,\ldots,n)$. This *n-dimensional* singular point has an eigenvalue of negative real number by ***Proposition 5*** (namely, it is a saddle point). Here, the value of k represents the depth of search. If k is set up to a large number, the precision of search is high but the computation time of search increases.

Then, we present the high-speed algorithm with k=3 in this paper, which has sufficient precision empirically. Here, some notations are defined.

Initial value vector of order parameter: $\xi(0)=(\xi_1(0),\xi_2(0),\ldots,\xi_n(0))$

Projection: $\pi_{i,j,k}(x_1,\ldots,x_n)=(x_i,x_j,x_k)$, $\{i,j,k\}\subseteq(1,\ldots,n)$

[*High-speed algorithm*]

Step 1: Search the n-3-*dimensional* singular points that have the same combination of signs as the signs of eigenvalues of a *n-dimensional* singular point.

Step 2: Search the n-2-*dimensional* singular points that are lower derivative singular points of the n-3-*dimensional* singular point founded in ***Step 1***.

Step 3: Approximate the hypercurves that connect origin and the singular points of ***Step 1, 2*** by straight lines.

Step 4: Approximate the hypersurfaces that connect the n-3-*dimensional* singular point with the n-2-*dimensional* singular points on the lines in ***Step 3*** by hyperplanes.

Step 5: Project an initial value vector of order parameter on 3-*dimensions* by using $\pi_{i,j,k}$. The number of extraction of 3-*dimensions* from *n-dimensions* is ${}_nC_k$.

Step 6: Choose an axis of the same region as the initial value vector projected on the region divided by hyperplanes.

Step 7: Repeat the ***Step 6*** ${}_nC_k$ times and count up the number of choices for every axis.

Step 8: Determine the axis with the maximal number of choices.

It is judged that the pattern according to the determined axis is recognized.

IV. EXPERIMENT

A. Experimental Environment

The environment of experiment is as follows:

a) Camera geometry is parallel, and camera parameter is known.

b) A stereo image has 320×240 pixels with 256 gray scales.

c) 30 stereo images including occlusion and reversal position are taken.

We evaluated the conventional method that numerically solved order parameter equations (9) and the proposed method with respect to computation time and matching precision for the 30 stereo images. For example, Fig. 6 shows the sample that include occlusion and reversal position. Here, the edges of objects are emphasized.

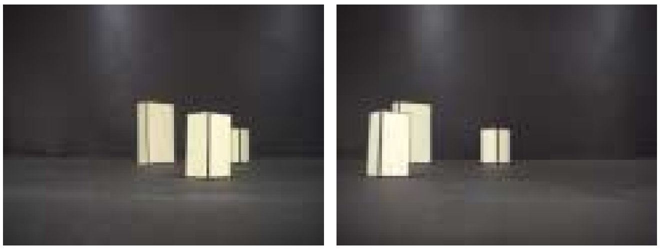

Fig. 6. Sample stereo image

B. Experimental Results

1) Evaluation about the computation time

First, the comparison of the computation time is shown in Fig. 7. The symbols △ and ● show the conventional method and the proposed method. And horizontal axis is the number of the feature points that can be matched. It is confirmed that the computation time of the proposed method remarkably decreases with the increase of the number of feature points. On the other hand, it turns out that the conventional method needs much computation time with the increase of the number of feature points.

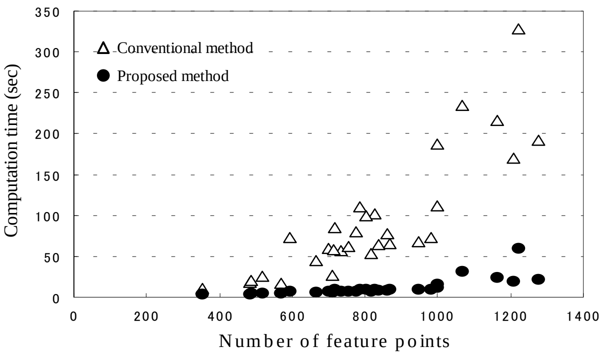

Fig. 7. The result of computation time

2) Evaluation about the matching precision

Secondly, the results of matching precision are shown in Fig. 8. The matching precision is defined as

$$T = \frac{\text{The number of correct correspondence points}}{\text{The number of possible correspondence points}} \times 100 . \tag{38}$$

Here, the number of possible correspondence points is counted up by a man. In Fig. 8, it is confirmed that the proposed method has obtained almost the same precision as the conventional method.

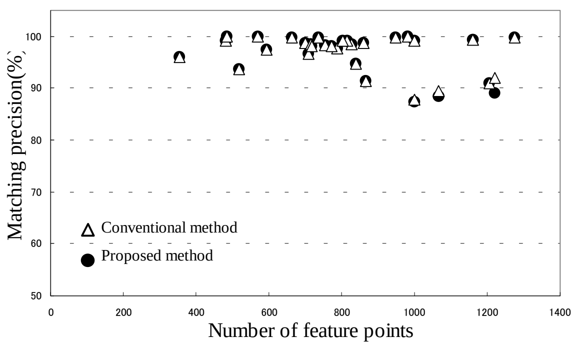

Fig. 8. The result of matching precision (CPU: Pentium II 400MHz)

V. CONCLUSIONS

We proposed a high-speed stereo matching algorithm based on Synergetics. The method does not numerically solve order parameter equations but determines the pattern by the approximated ridge hypersurface and initial values of order parameter. From the experimental results with 30 images, it was confirmed that the computation time remarkably decreases without the loss of matching precision. Hence, high precision and high-speed stereo matching algorithm was attained.

REFERENCES

[1] U. R. Dhond and J. K. Aggarwal, "Structure from Stereo-A Review", IEEE Trans. on SMC, Vol. 19, No.6, 1989, pp. 1489-1510.

[2] H.Maeda, S.Okada and T.Irie, "A New Method for Stereo Matching Problem in Computer Vision Using Synergetics", Proceedings of 1999 IEEE SMC,Vol.Ⅲpp503-508.

[3] H.Haken, *Synergetic Computers and Cognition*, Springer-Verlag, 1990.